J Appl Phycol (2014) 26:2097–2107
DOI 10.1007/s10811-014-0239-0

An experimental investigation on the multiphase flows and turbulent mixing in a flat-panel photobioreactor for algae cultivation

Zifeng Yang · Matteo del Ninno · Zhiyou Wen · Hui Hu

Received: 12 August 2013 / Revised and accepted: 6 January 2014 / Published online: 21 January 2014

Abstract Keeping an appropriate mixing state of the multiphase flows in photobioreactors (PBRs) is a key issue for the optimal design and operation of the PBRs. In the present study, an experimental investigation is conducted to quantify the turbulent mixing of multiphase flows inside a flat-panel PBR and its consequential effects on the performance of the PBR for algae cultivation. While a high-resolution particle image velocity (PIV) system is used to achieve detailed flow field measurements to quantify the unsteady behaviors of the multiphase flows and turbulent mixing inside the PBR, algae cultures are also grown in the same PBR under the same test conditions. Detailed flow field measurement results are correlated with the algae growth performance in order to elucidate the underlying physics and explore/optimize design paradigms. The measurement results reveal that even though the airflow rate that is supplied to the PBR plays a dominant role in determining the characteristics of the turbulent mixing in the PBR, the geometric positioning of the aeration inlets also significantly contributes to the turbulent mixing. These differences in turbulent mixing cause differences in algae productivity within the PBR, clearly effecting efficiency of the PBR.

Z. Yang · H. Hu
Department of Aerospace Engineering, Iowa State University, Ames, IA 50011, USA

H. Hu
e-mail: huhui@iastate.edu

M. del Ninno · Z. Wen
Department of Agricultural and Biosystems Engineering, Iowa State University, Ames, IA 50011, USA

Present Address:
Z. Yang (✉)
Department of Mechanical & Materials Engineering, Wright State University, Dayton, OH 45435, USA
e-mail: zifeng.yang@wright.edu

Keywords Flat-panel photobioreactor · Algae cultivation · Turbulence mixing · Multiphase flows · Particle image velocimetry (PIV) measurements

Introduction

Microalgae are an ideal source for liquid fuel production, as they can accumulate a large amount of lipid (oil) inside their cells and have very high biomass productivity (Wu and Merchuk 2004; Chisti 2007). Depending on the carbon number, the hydrocarbons can be processed into different types of jet fuels such as Jet A and JP-8 (Wijffels and Barbosa 2010, Hu et al. 2008). To date, most of the algal culture processes are performed in either open pond or closed loop photobioreactors (PBRs). While open pond PBRs are used to produce a large amount of algal biomass, closed loop PBRs have many inherent advantages such as well-controlled culture conditions (water, light, carbon dioxide, and nutrients), the capability to maintain high populations of the desired species, and high algal cell density. Among various designs of closed loop PBRs, flat-panel PBRs are commonly used because of the low capital investment, large surface-to-volume ratio, good light path, and high biomass productivity. Flat-panel PBRs are also relatively easy to scale up in the outdoor environment.

For the optimal design and operation of PBRs, turbulent mixing of multiphase flows has been recognized as an important factor in determining the overall performance of the PBRs (Weissman et al. 1988; Hu and Richmond 1996). Light intake rate, fluid dynamics, and algal metabolism are the three most important factors for algal growth. These three factors will influence each other, and the turbulent mixing process in PBRs is the core connecting the three factors. An appropriate mixing state of the multiphase flows in PBRs is the key for efficiently supplying CO_2, removing generated oxygen, providing alternating periods of light/dark cycle, evenly

distributing nutrients, and preventing cell sedimentation and thermal stratification. In a well-mixed PBR, local turbulences can carry the algal cells more or less randomly through the well-illuminated zones near the illumination sources and poorly illuminated zones remote from the light incidence. As a result, each individual cell will be exposed to the illuminating light in a statistical light/dark cycle. A well-mixed bioreactor is also necessary to prevent the algal cells from settling or attaching to the reactor walls and to enhance gas exchange so that the algal cells will not be limited by CO_2 supply and/or inhibited by excess O_2 accumulation. However, an intensive mixing may result in a high shear stress, which may cause physical damages to algal cells, hence limiting algal growth (Silva et al. 1987; Schultz 2000). Therefore, to keep an appropriate mixing state is a key issue for the optimal design and operation of a PBR.

Weissman et al. (1988) conducted a pioneer study to investigate the effects of mixing on algal growth in PBRs. Hu and Richmond (1996) found that as the cell density increases, the dependence of cell density on the mixing in the PBR was found to become significant, and a good mixing state would result in a better density of algal cells. More recently, a number of studies have also been conducted to evaluate the effects of turbulent mixing on the algal growth in various PBRs (Kliphuis et al. 2010; Barbosa et al. 2003; Janssen et al. 2000; Bacock et al. 2002). However, most of those previous studies treated PBRs as black boxes, without conducting detailed investigations on the distributions of various relevant physicochemical parameters such as light intensity, CO_2 and O_2 concentration, and temperature distribution in the PBRs. In practice, there will always be inevitably some "dead zones" which cause depletion of nutrients without replenishment, entrapment of algal cells, CO_2 inaccessibility, O_2 over accumulation, and temperature stratification. One of the major challenges in the optimal design and operation of PBRs for algal cultivation is the lack of in-depth understanding of the characteristics of multiphase flows and turbulent mixing in PBRs.

In the present study, an experimental analysis was conducted to quantify the characteristics of the turbulent mixing of multiphase flows in a flat-panel PBR. A high-resolution particle image velocimetry (PIV) system was used to achieve whole-field measurements to quantify the transient behaviors of both air bubbles and liquid-phase fluid flows in the PBR simultaneously. In addition to quantifying the flow velocity distribution of the recirculating fluid flows in the PBR, the travel paths and rising velocities of the air bubbles were also investigated under different test conditions. Algal cultures were also grown in the same flat-panel bioreactor under the same test conditions as those for the flow measurements. The measured mixing characteristics of the multiphase flows in the PBR are correlated with the algal growth performance to elucidate the underlying physics in order to develop a practical protocol for improved algae biomass growth performance.

Materials and methods

Setup of the flat-panel PBR

Figure 1 shows the schematic and photo of the flat-panel PBR model. The model is made of transparent Plexiglas with the dimension of 610 mm×610 mm×50 mm (length, height, and width). The working fluid is water with a volume of 15.45 L. Compressed air was supplied to the PBR through the aeration pores with a diameter of 0.9 mm on the bottom of the reactor. As shown in Fig. 2, while a flow meter was used to monitor the airflow rate, an air distributor was designed to evenly distribute the compressed air to the aeration pores connected through the small Tygon tubing. By pinching or releasing the tubing, the airflow was distributed into the PBR through aeration pores in three different configurations, i.e., (a) configuration #1, through three pores concentrated in the middle of the PBR with a spacing of L=92 mm between pores; (b) configuration #2, through three pores distributed evenly with a

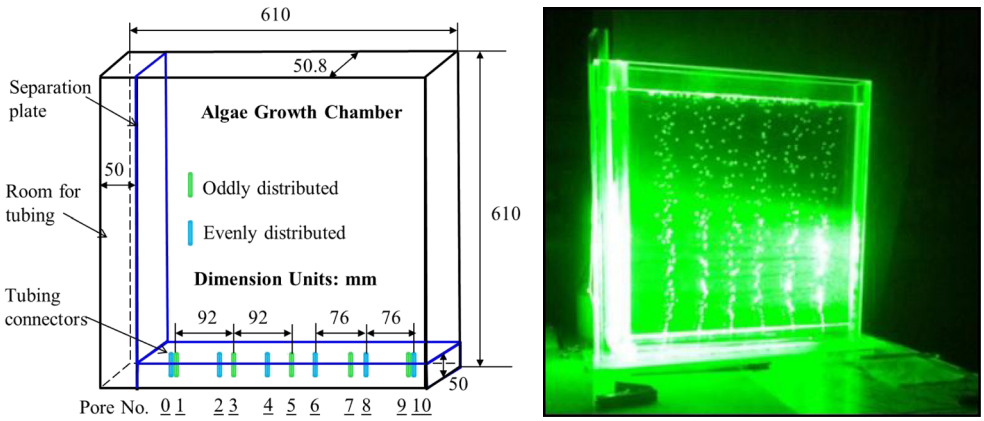

(a). The schematic of the PBR model (b). Picture of the PBR model

Fig. 1 The flat-panel PBR model used in the present study. **a** The schematic of the PBR model. **b** Picture of the PBR model

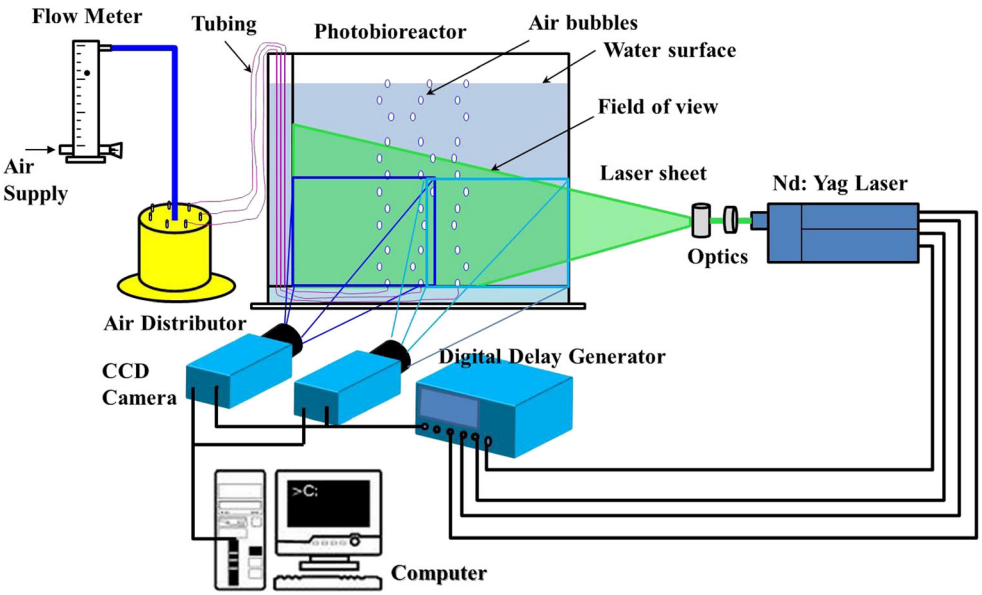

Fig. 2 Experimental setup for the flow field measurements

wider spacing of L=228 mm between pores; (c) configuration #3, through six pores distributed evenly with a distance of L= 76 mm between pores; and (d) configuration #4, through all the 11 pores. Table 1 lists the tested cases of the present study with the corresponding airflow rate and aeration configurations. Further details about the PBR model, the experimental setup and selection of test cases are available in the study of Ninno (2012).

Experimental setup for the flow field measurements

A high-resolution digital PIV system was used in the present study to achieve detailed flow field measurements. Figure 2 shows the schematic of the experimental setup for the PIV measurements. The water inside the PBR was premixed with ~10 μm silver-coated hollow glass spheres as the tracers. Illumination was provided by a double-pulsed Nd:YAG laser (NewWave Gemini 200) adjusted on the second harmonic and emitting two pulses of 200 mJ at the wavelength of 532 nm. The laser beam was shaped to a sheet by a set of spherical and cylindrical lenses. The thickness of the laser sheet in the measurement region was about 1.0 mm. Two high-resolution, 12-bit couple-charged device (CCD) cameras (resolution of 1,600×1,200 pixels, PCO1600, Cooke Corp.) were used for PIV image acquisition to ensure high spatial resolutions. The cameras and lasers were connected to a workstation via a digital delay generator (Berkeley Nucleonics, Model 565), which controlled the timing of the laser illumination and the image acquisition.

Data processing

The velocity distributions of both the liquid flow and the rising air bubbles in the PBR were derived simultaneously from the acquired PIV images. As shown in Fig. 3a, bright air bubbles and tracer particles within the liquid can be seen in the acquired raw image. The positions and shapes of the air bubbles can be extracted from raw images through an image processing procedure similar as those used by Lindken and Merzkirch (2000) and Liu et al. (2005). Figure 3b shows the images of the air bubbles extracted from the acquired raw images given in Fig. 3a. Based on time sequences of acquired images, the moving velocities of the air bubbles in the PBR were determined by using a particle tracking velocimetry (PTV) method

Table 1 The controlling flow parameters of the cases studied

Test case no.	Input airflow rate (mL min^{-1})	Number of aeration pores used	The pores used for the aeration at the bottom of PBR
1	200	3	3, 5, 7
2	500	3	3, 5, 7
3	500	3	0, 5, 10
4	500	6	0, 2, 4, 6, 8, 10
5	800	3	3, 5, 7
6	1,600	11	0, 1, 2, 3, 4, 5, 6, 7, 8, 9, 10

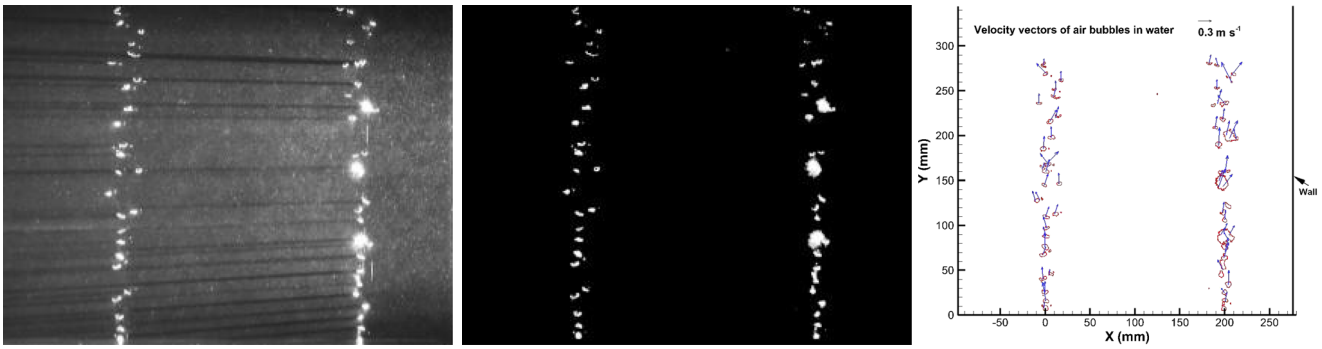

(a) Acquired raw image (b) Instantaneous image of air bubbles (c) Velocity of the air bubbles

Fig. 3 An image processing procedure to determine the size and positions of the air bubbles. **a** Acquired raw image. **b** Instantaneous image of air bubbles. **c** Velocity of the air bubbles

(Ohmi and Li 2000). Figure 3c gives an example to show the positions and shapes of the air bubbles along with the corresponding instantaneous velocities of the air bubbles.

After removing air bubbles from the original PIV raw images, a cross-correlation-based PIV image processing technique was used to derive the instantaneous velocity vectors of the tracer particles in the fluid (Adrian 1991, 2005). The cross-correlation technique involves successive frames of patterns in an interrogation window of 32×32 pixels. It should be noted that the averaged equivalent diameter of the air bubbles was found to be about 11 pixels in the acquired PIV images, which is much smaller than the size of the interrogation windows. By setting this size for PIV image processing, only a small amount of spurious vectors (i.e., <2 %) was found in the instantaneous frames of liquid flow velocity distributions. In the present study, an effective overlap of 50 % of the interrogation windows was employed in the PIV image processing for the liquid flow. After the instantaneous velocity vectors (u_i and v_i) were determined, the vorticity (ω_z) was derived. The distributions of the ensemble-averaged flow quantities such as the mean velocity U and the in-plan turbulent kinetic energy of the fluid flow ($\mathrm{TKE} = 0.5 \times \left(\overline{u'}^2 + \overline{v'}^2\right)$) were obtained from a sequence of about 1,000 frames of instantaneous PIV measurements. The measurement uncertainty level for the velocity vectors was estimated to be within 2 %, while the uncertainties for the measurements of ensemble-averaged flow quantities such as turbulent kinetic energy (TKE) distributions were about 5 %.

Algal culture experiment

In the present study, algae cultivation experiments were performed using the same PBR and under the same test condition as described above to grow *Scenedesmus dimorphus*. This was to correlate the flow characteristics and turbulence mixing

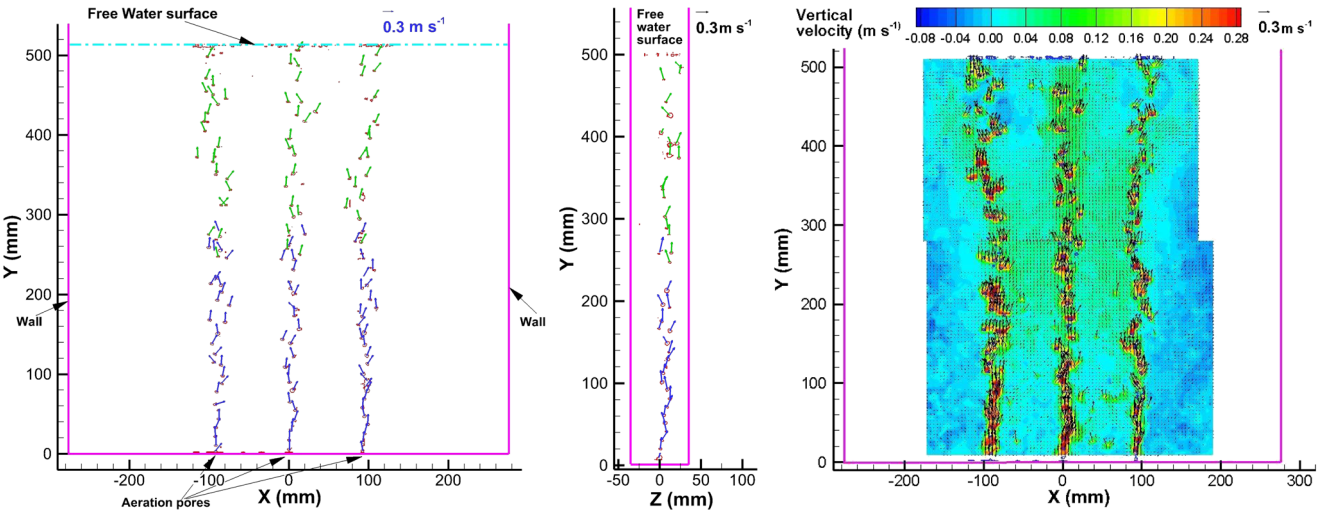

(a) (b) (c)

Fig. 4 A typical instantaneous PIV measurement results for the test case #1. **a** Instantaneous velocity of air bubbles in the *XY* plane. **b** Instantaneous velocity of air bubbles in the *YZ* plane. **c** The corresponding instantaneous flow velocity inside the PBR

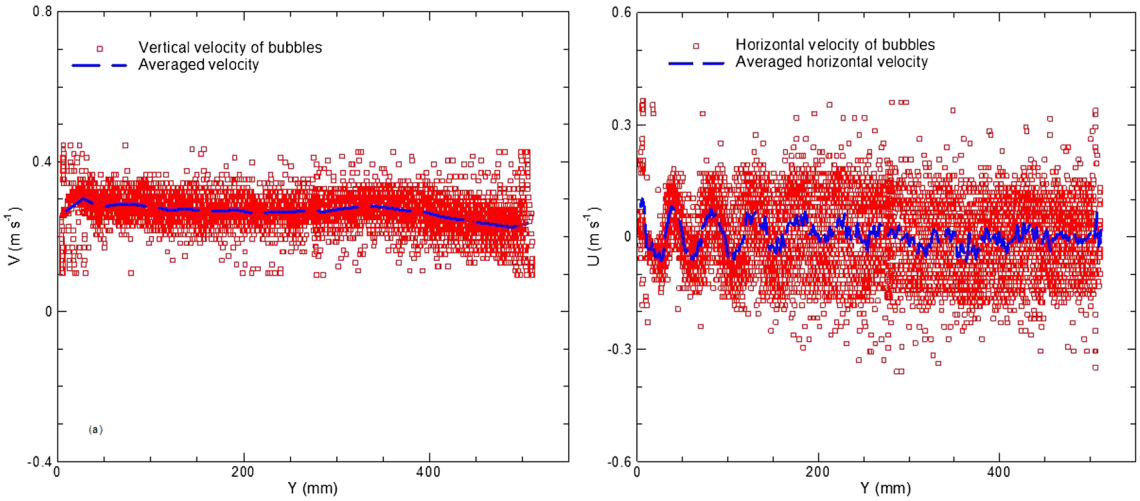

(a). vertical velocity component; (b). horizontal velocity component.

Fig. 5 Measured vertical and horizontal velocity components of the rising air bubbles exhausted from the aeration pore #3 for test case #1. **a** Vertical velocity component. **b** Horizontal velocity component

inside the PBR with the algae growth performance during cultivation. The liquid medium for the culture was selected with a pH value of about 7.0. The illumination source was provided by a 60-W cool white plus fluorescent light at 110–120 μmol photons m^{-2} s^{-1}. The concentration of CO_2 in the airflow supplied to the PBR was about 2 %. A standard algae cultivation procedure has been followed up carefully during experiments including procedural maintenance and careful PBR cleaning after each test trial by using diluted bleach in order to prevent the microalgae culture from contaminations of bacteria. Further information about the experimental setup and the lab procedure can be found in the study of Ninno (2012). Following the work of Myers et al. (2013), the algal cell growth performance in the PBR was monitored by measuring the optical density of the solution in the PBR with a light beam of wavelength at 685 nm. Optical density, measured using a spectrophotometer, can be used as an index of the concentration of algal cells in a suspension (Myers et al. 2013).

Results

The motions of the air bubbles and fluid flows in the PBR

Figure 4 shows typical instantaneous PIV measurement results in terms of instantaneous moving velocity of the air bubbles (both front and side views) and the corresponding liquid-phase flow velocity vectors inside the PBR. The air bubbles were stumping and meandering around to generate

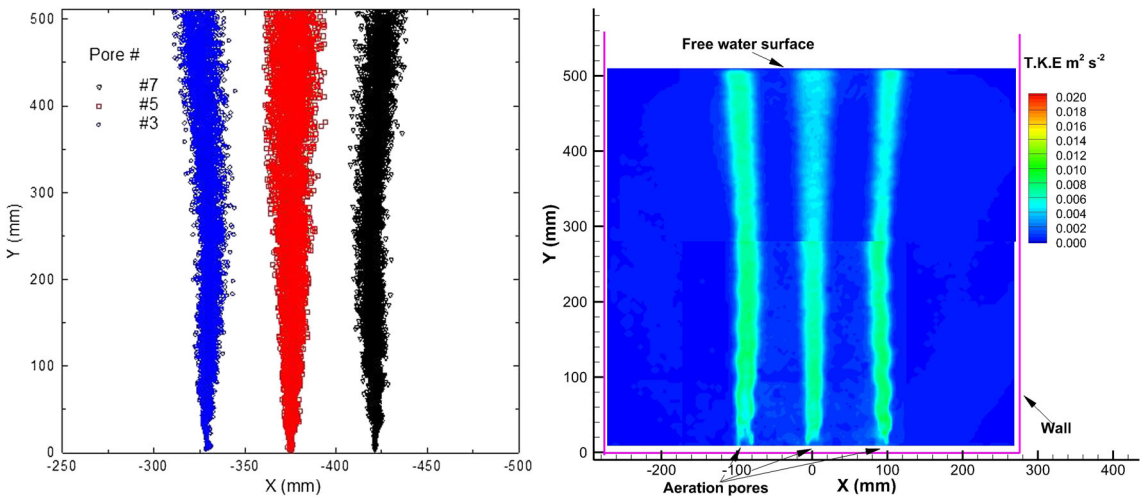

(a). Accumulative distribution of air bubbles (b). TKE distribution of the fluid flow

Fig. 6 The measurement results for test case #1. **a** Accumulative distribution of air bubbles. **b** TKE distribution of the fluid flow

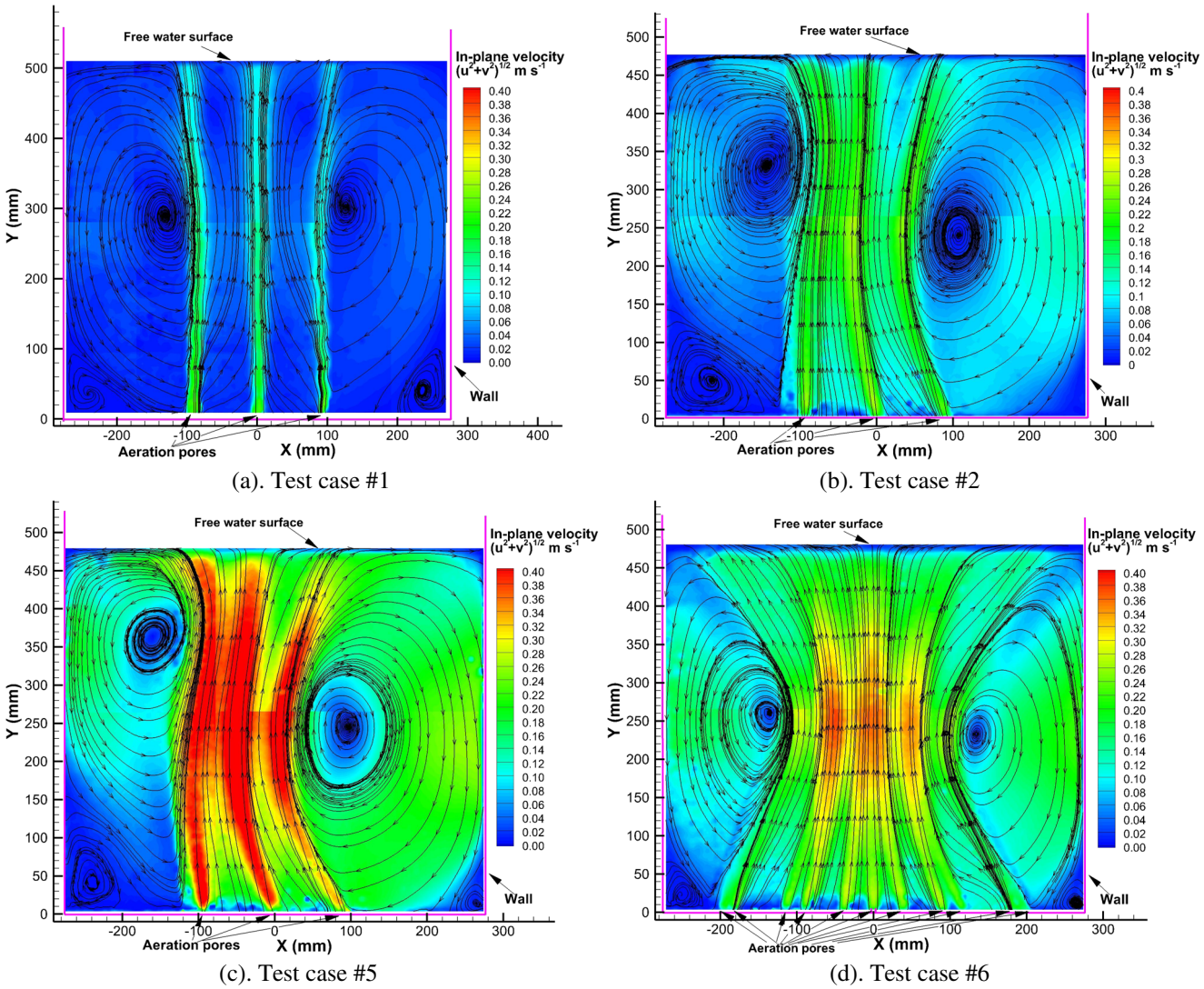

Fig. 7 The flow patterns inside the PBR under different test conditions. Test cases **a** #1, **b** #2, **c** #5, and **d** #6

zigzag trajectories while rising up from the bottom of the PBR. Corresponding to the upward motion of the air bubble, the liquid on the top of the rising bubble was pushed upwards, and the liquid behind the rising air bubble was pulled up by entrainment. It induced high upward velocity of the liquid in the region near the rising air bubble column as shown clearly

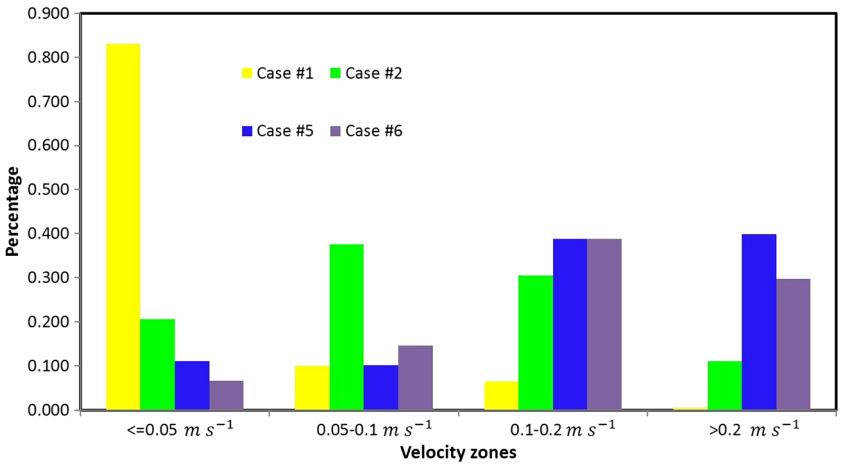

Fig. 8 Statistics of the different velocity zones vs. the airflow rate supplied to the PBR

Table 2 The statistics of the flow properties for test cases #1, #2, #5, and #6

Test case no.	Airflow rate (mL min^{-1})	Averaged flow velocity in the PBR (m s^{-1})	Averaged TKE in the PBR (m^2 s^{-2})
1	200	0.0353	0.00107
2	500	0.106	0.00389
5	800	0.212	0.01167
6	1,600	0.163	0.00832

in Fig. 4c. Similar phenomena were also reported by Lindken and Merzkirch (2000) and Liu et al. (2005) in characterizing the behavior of gaseous bubbles rising in water.

According to the work of Saffman (1956a, b), air bubbles with a volume equivalent diameter between 2.0 and 4.6 mm would mostly travel in zigzag trajectories. However, if air bubbles experience sufficiently external disturbances, the trajectories would change from zigzag to spiral, without any preference in a particular plane. The similar phenomena were observed in the present study. Air bubbles showed zigzag trajectories at the beginning with $Y/L<2.0$. Then, the air bubbles were found to be characteristically wobbling in the fluid flow

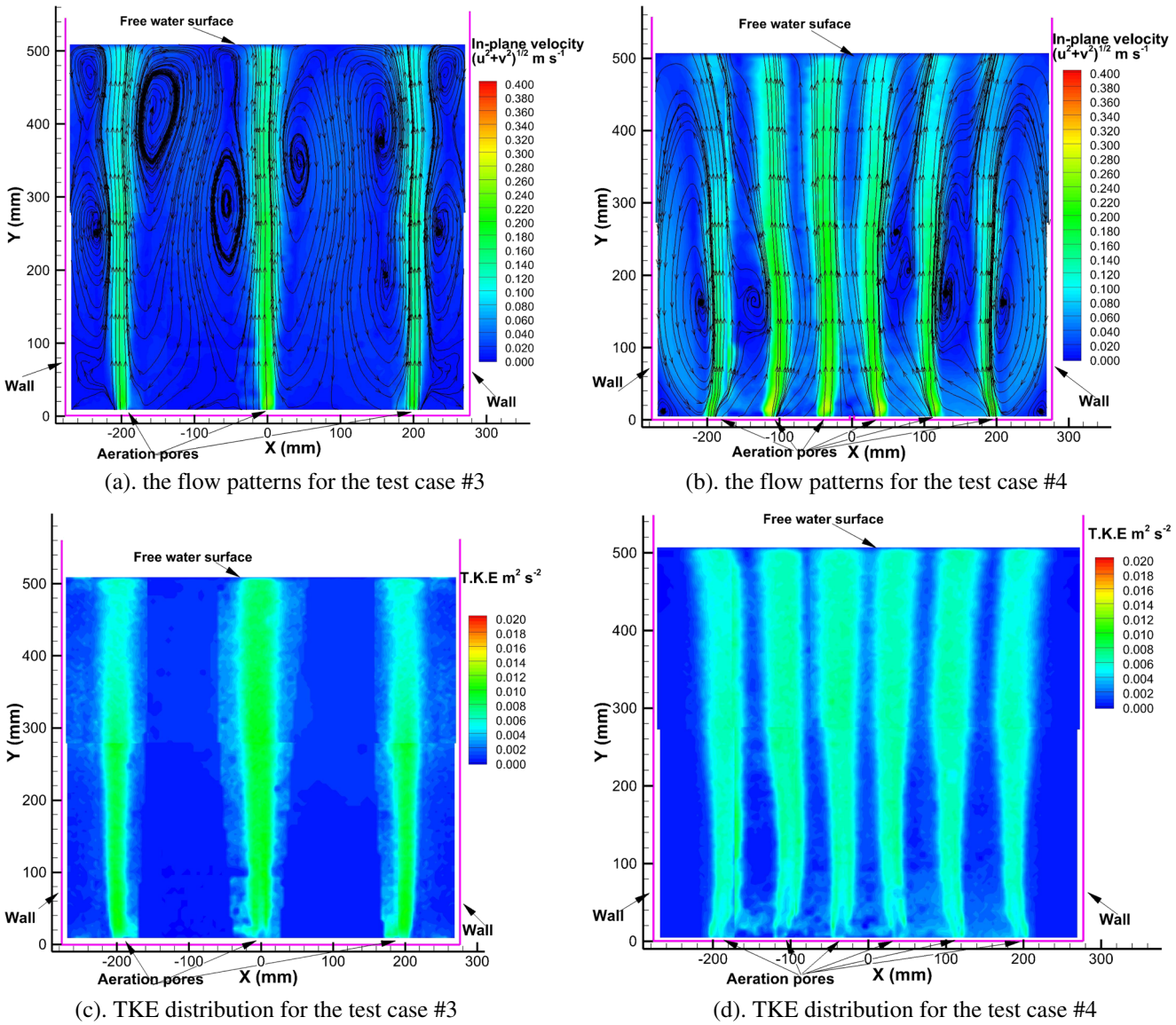

(a). the flow patterns for the test case #3

(b). the flow patterns for the test case #4

(c). TKE distribution for the test case #3

(d). TKE distribution for the test case #4

Fig. 9 The flow patterns and the TKE distributions inside the PBR for the test cases #3 and #4. **a** The flow patterns for the test case #3. **b** The flow patterns for the test case #4. **c** TKE distribution for the test case #3. **d** TKE distribution for the test case #4

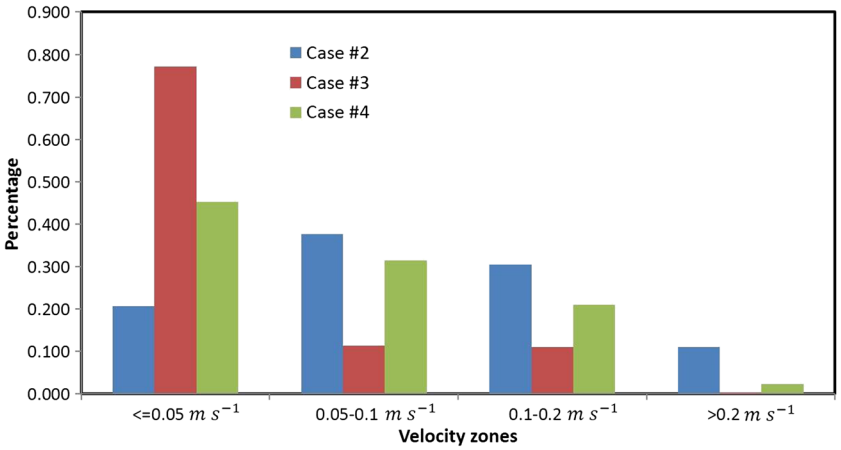

Fig. 10 Statistics of the different velocity zones in the PBR vs. the aeration arrangement

(i.e., in a spiral motion) at further downstream. However, after traveling for a certain distance, the motion of the air bubbles would become more random in the horizontal plane, which is mainly due to the high turbulence level in the region. Such random motion in the region would also weaken the entrainment effect and results in more drag acting on the bubbles.

Figure 5 shows the histogram of the instantaneous vertical and horizontal velocity components of the rising air bubbles exhausted from the aeration pore #3 in case #1. The time-averaged velocity of air bubbles at different elevations was also given in the plots as the broken lines. The overall averaged rising velocity of air bubbles was about 0.27 m s^{-1}, while the local rising velocity of air bubbles increased rapidly at beginning and then almost kept as a constant until $Y/L \approx 3.7$, where L is the distance between the aeration pores. The averaged vertical velocity of the air bubbles decreased slightly with the increasing height above $Y/L \approx 3.7$.

Figure 6a shows center locations of air bubbles generated in the PBR for case #1 during a time interval of 60 s. Figure 6b presents the corresponding TKE distribution of the liquid-phase flows in the PBR. It can be observed that the regions with high TKE in the fluid flow correlate with the appearance of air bubble columns in the PBR very well, i.e., the regions with high TKE in the fluid flow were dominated by the pseudo-turbulence due to the appearance of the air bubbles.

The effects of the airflow rate on the turbulent mixing inside the PBR

The airflow containing CO_2 supplied to the PBR is a key factor that affects the growth rate of algal cells in the PBR (Weissman et al. 1988; Vunjak-Novakovic et al. 2005; Wang et al. 2008). Therefore, the effects of the airflow rate on the turbulent mixing of the multiphase flows in the PBR and the consequential effects on microalgae cultivation were investigated. Figure 7 shows the patterns of the fluid flow inside the PBR for cases #1, #2, #5, and #6. As the airflow rate increases, while the strength of the fluid flows inside the PBR increases monotonically, the flow pattern was found to be quite similar in general. Two large circulation zones were formed in both sides with fluid moving upward in the middle and downward at two sides of the PBR. Smaller recirculation zones, called dead zones, were formed near the bottom corners of the PBR. The interaction between the neighboring air bubble columns became much more obvious and violent, as the airflow rate increases. As the airflow rate supplied to the PBR increases to Q=500 mL min^{-1} or higher, the fluid flow inside the PBR became very unsteady, and the mixing of the multiphase flows inside the PBR turned out to be intensive.

As described in the study of Marshall and Huang (2010), the mean fluid velocity in a PBR has been used as a quantitative parameter to describe the mixing performance of the PBR. However, the method is plagued by oversimplification of fluid dynamics. Instead of using a single value of the mean flow velocity, the flow field in the PBR was fractioned into four velocity zones in order to represent the turbulent mixing more accurately. We defined v<0.05 m s^{-1} as the very low-velocity zone, $0.05 \le v \le 0.10$ m s^{-1} as the low-velocity zone, $0.10 \le v \le 0.20$ m s^{-1} as the medium-velocity zone, and v> 0.20 m s^{-1} as the high-velocity zone. In general, a larger area percentage of the high-velocity zone indicates a better mixing performance of the PBR. Figure 8 shows the comparisons of

Table 3 The comparison of the statistics of the flow properties for cases #2, #3, and #4

Test case no.	Airflow rate (mL min^{-1})	Averaged flow velocity in the PBR (m s^{-1})	Averaged TKE in the PBR (m^2 s^{-2})	Normalized TKE
2	500	0.106	0.00389	0.347
3	500	0.038	0.00242	1.698
4	500	0.068	0.00328	0.710

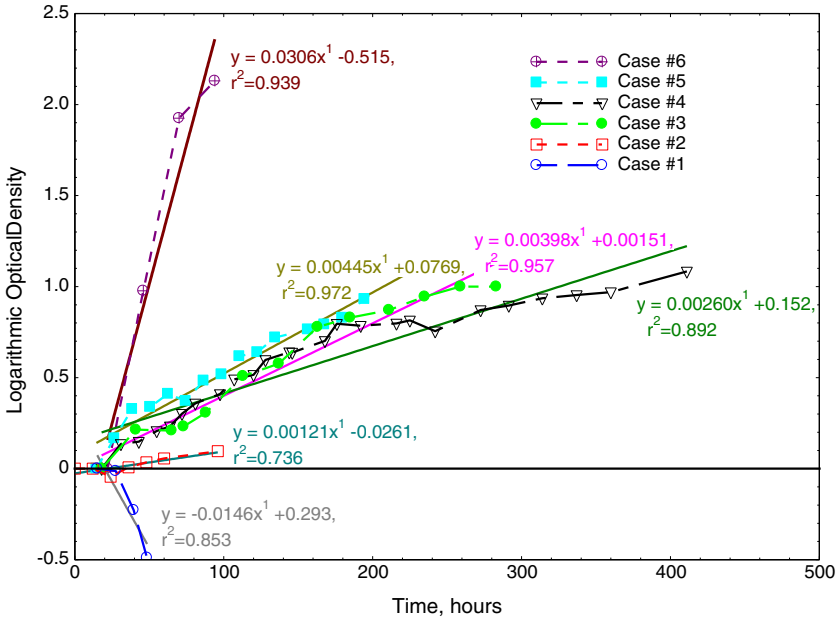

Fig. 11 Algal growth under different test conditions

the statistics of different velocity zones. Test case #5 has much higher percentages of high-velocity zones compared with those of cases #2 and #1. The expectations were confirmed quantitatively by the algae cultivation experiments, which will be presented and discussed later. It should be also noted that, although a large mean velocity or a higher percentage of high-velocity zones would indicate a better mixing, it may not be suitable to solely use the mean flow velocity or the percentages of the high-velocity zones to determine the overall mixing efficiency, especially when comparing with the test cases with different aeration arrangements, for example, case #6.

In addition to mean flow velocity, the TKE of the fluid flow was also recognized as an index to quantify the turbulence mixing of the multiphase flows in a PBR (Thomas and Gibson 1990; Yu et al. 2009). Both the averaged flow velocity and TKE of the fluid flow were calculated (Table 2). As expected, with the same aeration arrangements, both the averaged flow velocity and TKE inside the PBR were found to increase with the increasing airflow rate supplied to the PBR. The trend derived from the present study was found to agree well with those reported in Yu et al. (2009) and Marshall and Huang (2010).

The effects of the aeration arrangements on the turbulent mixing inside the PBR

Even though the total amount of the airflow supplied to the PBR was kept the same during the experiment, characteristics of the turbulent mixing inside the PBR varied greatly with various aeration arrangements, which can be observed from the flow streamlines shown in Fig. 9a, b. Figure 9c, d presents the corresponding turbulent kinetic energy distributions in the PBR for cases #3 and #4. As expected, the distributions of the TKE were found to be well correlated with the pseudo-turbulent flows induced by the rising air bubbles. Compared with those of case #3, the regions with high TKE values were found to be occupying much more area in the PBR for test case #4 due to more contacts between air bubble columns and flows.

The statistics of the percentages of the four velocity zones for test cases #2, #3, and #4 are presented in Fig. 10. Case #2 was found to have the highest percentages of the high-velocity zones among the three test cases, and test case #4 had a higher percentage of the high-velocity zones than test case #3. As aforementioned, in addition to using mean flow velocity, turbulent kinetic energy was also used as an index to quantify the turbulent mixing of the multiphase flows. Based on the PIV measurements, the averaged flow velocity and the averaged TKE values in the PBR were calculated for the test cases (Table 3). Corresponding to the statistics of four velocity zones in the PBR given in Fig. 10, while test case #2 was found to have the highest averaged flow velocity and TKE values among the three compared test cases, case #4 was found to have a higher averaged flow velocity and TKE values compared with case #3.

The normalized TKE was also obtained by normalizing the averaged TKE using the averaged velocity in the PBR (Table 3). The lowest normalized TKE was found in case #2, although the value of averaged TKE is the highest. In correlation with the results in Fig. 11, it might be concluded that with the same flow rate, the distribution of bubbles that can generate the highest normalized TKE could produce the highest mixing efficiency and the highest growth rate as a consequence.

Therefore, case #3 generates the highest growth rate, and case #2 generates the lowest growth rate. This indicates that for the same velocity, the more the turbulence, the better is the mixing efficiency.

Effects of turbulent mixing on the algae growth performance in algae cultivation

Figure 11 shows the results of algae cultivation experiments. The slope of the curve fit serves as an index of the growth rate, while the intercept in the curve fit can be ignored. As shown in Fig. 11, generally, a higher airflow rate supplied to the PBR would result in a better algae growth in general. For case #1, since the airflow rate supplied to the PBR is very low, the cells of the microalgae tended to stick together and/or settle on the bottom plate or side walls of the PBR. As a result, the cell concentration of microalgae in the PBR decreases with time. As the airflow rate increases to Q=500 mL min^{-1} for case #2, it prevented the settling of algal cells, but the airflow rate is still not high enough to reach an optimum mixing state in the PBR for a noticeable growth rate of microalgae. As shown in Fig. 7d, since relatively large stagnation zones still existed, significant sedimentations of algal cells were found in these zones. As a result, the density of the microalgal cells increased very slowly. For case #5, as shown in Fig. 7c, the turbulent mixing inside the PBR became much more intense due to the higher airflow rate and stronger interactions among air bubble columns. As a result, the growth of algal cells increased at a much faster rate. For case #6, since the airflow was supplied to the PBR evenly through 11 aeration pores with the highest airflow rate of Q=1,600 mL min^{-1} (Fig. 7d), strong interactions among the air bubble columns induce strong recirculation flows to promote the turbulent mixing inside the PBR. Therefore, case #6 had the best algae growth rate among all six cases.

While the airflow rate was kept in constant, the configuration of the aeration arrangement is expected to affect the algae growth rate considerably. The algae growth rate for case #2 was found to be quite low due to large dead zones near the corners of the PBR. For case #3, since the airflow was supplied into the PBR through three widely distributed aeration pores, the fluid flows induced by the three well-separated air bubble columns promoted turbulent mixing to eliminate the dead zones in the PBR. As a result, a much faster algae growth rate was achieved for case #3. For case #4, although the airflow was distributed more uniformly into the PBR through six aeration pores, the actual airflow rate supplied to each of the aeration pores becomes much lower. Therefore, the algae growth profile for case #4 shows a similar trend as that of case #3 at the beginning, but slowing down after 140 h.

Discussion

In the present study, the motions of air bubbles exhausted from the bottom were characterized in order to assess the effects of the rising air bubbles on the behavior of the fluid flows and turbulent mixing inside the PBR. Driven by the buoyancy force, the air bubbles move upward in zigzag trajectories at the early stage and then in spiral motions further downstream. Corresponding to the upward motions of the air bubbles, strong upward turbulent fluid flows are induced which result in the intensive turbulent mixing in the PBR. The present study confirmed that the algal growth performance of the PBR can be correlated with the mixing performance of the multiphase flows inside the PBR very well. The airflow rate supplied to the PBR presents a dominant effect on the flow characteristics and turbulence mixing inside the PBR, thereby the algae growth performance. Within the range of the present study, the algae growth rate increases monotonically with the airflow rate. An airflow rate of 800 mL min^{-1}, i.e., case #3, produced the best growth for the same centered distribution of pores. In addition to the airflow rate, the configuration of the aeration arrangement significantly affects the turbulent mixing and the algae growth of the PBR, which did not draw much attention in the previous studies. The best performance was observed for the widely distributed pores, case #3. The detailed flow field measurements given in the present study can also be used for the development of theoretical models as well as validation and verification of CFD studies to simulate the multiphase flows in bioreactors.

References

Adrian RJ (1991) Particle-imaging techniques for experimental fluid mechanics. Annu Rev Fluid Mech 23:261–304

Adrian RJ (2005) Twenty years of particle image velocimetry. Exp Fluids 39:159–169

Babock RW, Malda J, Radway JC (2002) Hydrodynamics and mass transfer in a tubular airlift photobioreactor. J Appl Phycol 14:169–184

Barbosa MJ, Janssen M, Ham N, Tramper J, Wijffels RH (2003) Microalgae cultivation in air-lift reactors: modeling biomass yield and growth rate as a function of mixing frequency. Biotechnol Bioeng 82:170–179

Chisti Y (2007) Biodiesel from microalgae. Biotechnol Adv 25:294–306

Hu Q, Richmond A (1996) Productivity and photosynthetic efficiency of *Spirulina platensis* as affected by light intensity, algal density and rate of mixing in a flat plate photobioreactor. J Appl Phycol 8:139–145

Hu Q, Sommerfeld M, Jarvis E, Ghirardi M, Posewitz M, Seibert M, Darzins A (2008) Microalgal triacylglycerols as feedstocks for biofuel production: perspectives and advances. Plant J 54:621–639

Janssen M, Janssen M, de Winter M, Tramper J, Mur LR, Snel J, Wijffels RH (2000) Efficiency of light utilization of *Chlamydomonas reinhardtii* under medium-duration light/dark cycle. J Biotechnol 78:123–137

Kliphuis AMJ, de Winter M, Vejrazka C, Martens DE, Janssen M, Wijffels RH (2010) Photosynthetic efficiency of *Chlorella sorokiniana* in turbulently mixing short light-path photobioreactor. Biotechnol Prog 26:687–696

Lindken R, Merzkirch W (2000) Velocity measurements of liquid and gaseous phase for a system of bubbles rising in water. Exp Fluids 209:S194–S201

Liu Z, Zheng Y, Jia L, Zhang Q (2005) Study of bubble induced flow structure using PIV. Chem Eng Sci 60:3537–3552

Marshall JS, Huang Y (2010) Simulation of light-limited algae growth in homogeneous turbulence. Chem Eng Sci 65:3865–3875

Myers JA, Curtis BS, Curtis WR (2013) Improving accuracy of cell and chromophore concentration measurements using optical density. BMC Biophys 6:1–15

Ninno MP (2012) Investigation of turbulent multiphase flows in a flat panel photobioreactor and consequent effects on microalgae cultivation; using computational fluid dynamics (CFD) simulation and particle image velocimetry (PIV) measurement. MSc Thesis, Iowa State University

Ohmi K, Li HY (2000) Particle-tracking velocimetry with new algorithms. Meas Sci Technol 11:603–616

Saffman PG (1956a) On the rise of small air bubbles in water. J Fluid Mech 1:249–275

Saffman PG (1956b) On the motion of small spheroidal particles in a viscous liquid. J Fluid Mech 1:540–553

Shultz MP (2000) Turbulent boundary layers on surfaces covered with filamentous algae. J Fluids Eng 122:357–363

Silva HJ, Cortinas T, Ertola RJ (1987) Effect of hydrodynamic stress on *Dunaliella* growth. J Chem Technol Biotechnol 40:41–49

Thomas WH, Gibson CH (1990) Effects of small-scale turbulence on microalgae. J Appl Phycol 2:71–77

Vunjak-Novakovic G, Kim Y, Wu X, Berzin I, Merchuk J (2005) Air-lift bioreactors for algal growth on flue gas: mathematical modeling and pilot-plant studies. Ind Eng Chem Res 44:6154–6163

Wang B, Li Y, Wu N, Lan C (2008) CO_2 bio-mitigation using microalgae. Appl Microbiol Biotechnol 79:707–718

Weissman JC, Goebel RP, Benemann J (1988) Photobioreactor design: mixing, carbon utilization, and oxygen accumulation. Biotechnol Bioeng 31:336–344

Wijffels R, Barbosa M (2010) An outlook on microalgal biofuels. Science 329:796–799

Wu X, Merchuk JC (2004) Simulation of algae growth in a bench scale internal loop airlift reactor. Chem Eng Sci 59:2899–2912

Yu G, Li Y, Shen G, Wang W, Lin C, Wu H, Chen Z (2009) A novel method using CFD to optimize the inner structure parameters of flat photobioreactors. J Appl Phycol 21:719–727